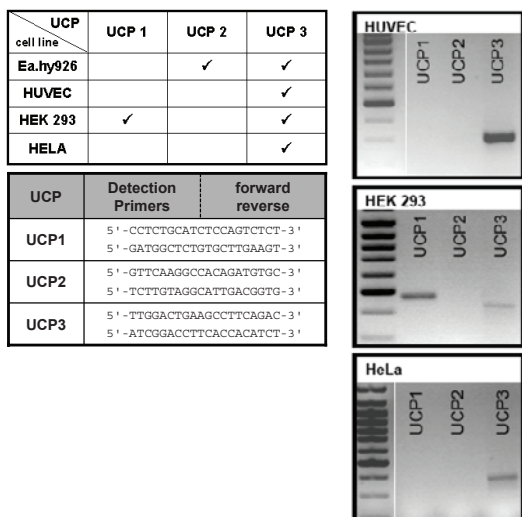
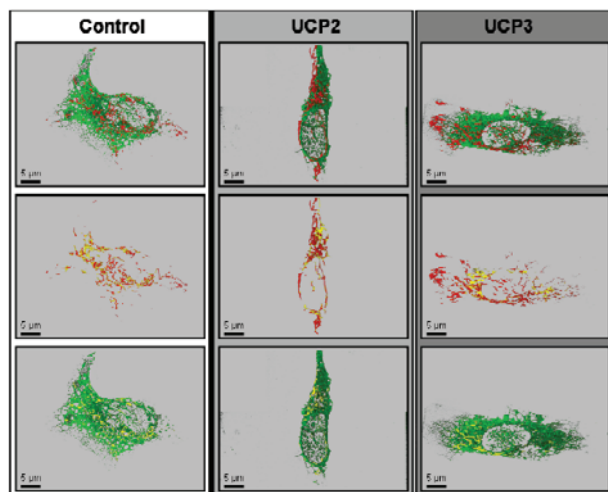


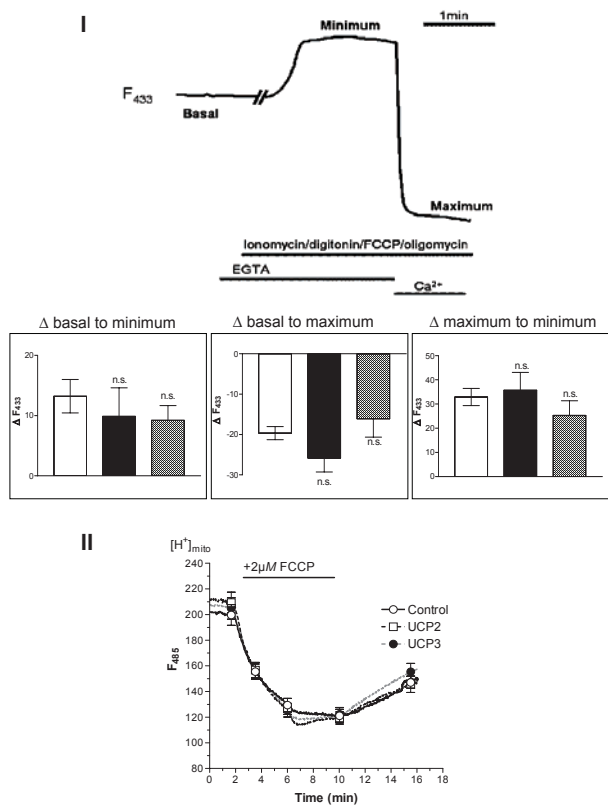
Suppl. Fig. 1a



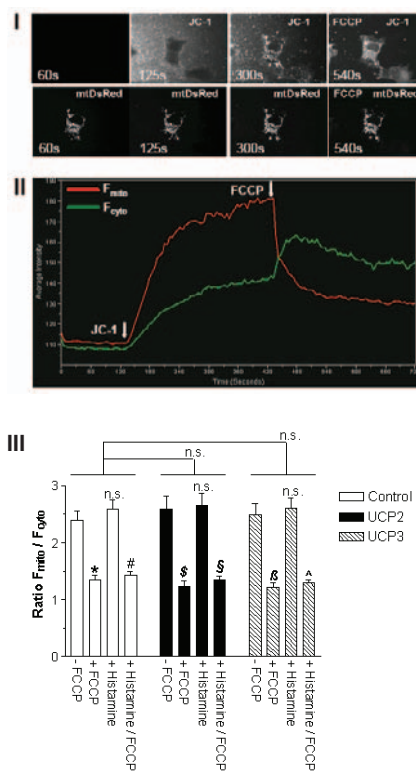
Suppl. Fig. 1b



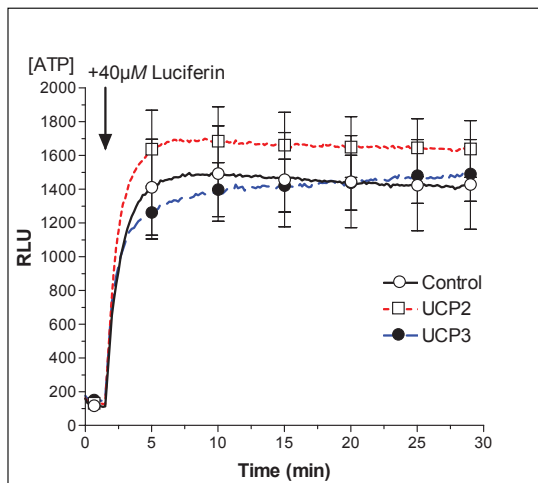
Suppl. Fig. 1c



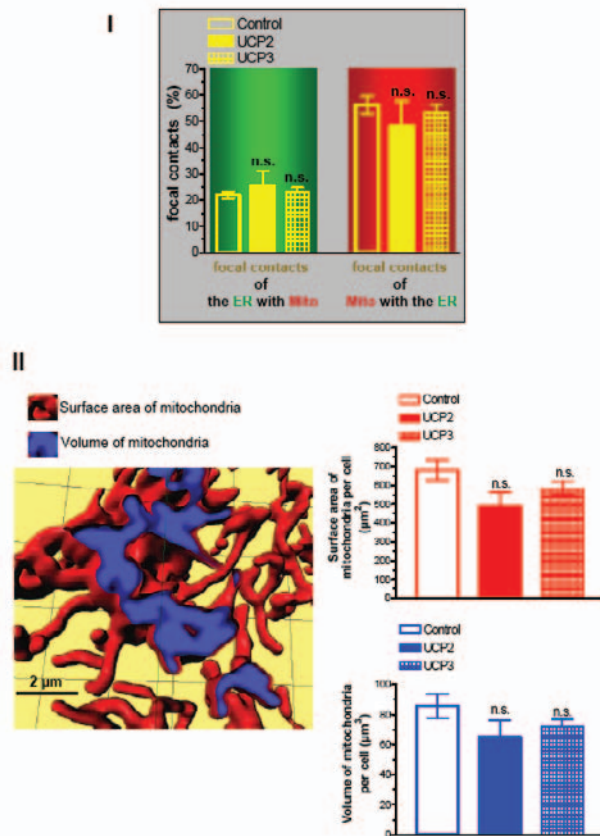
Suppl. Fig. 1d



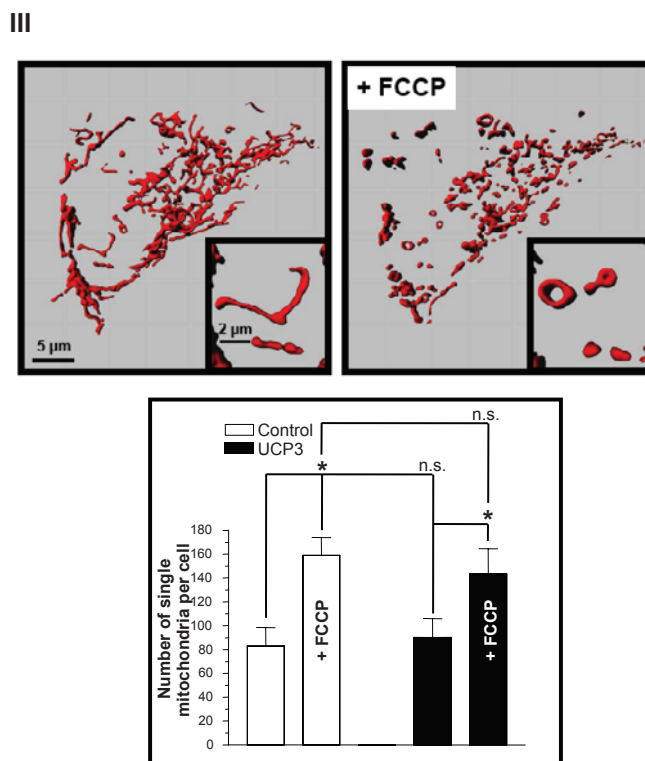
Suppl. Fig. 1e



Suppl. Fig. 1f



Suppl. Fig. 1g



Suppl. Fig. 1h

Suppl. Fig. 1

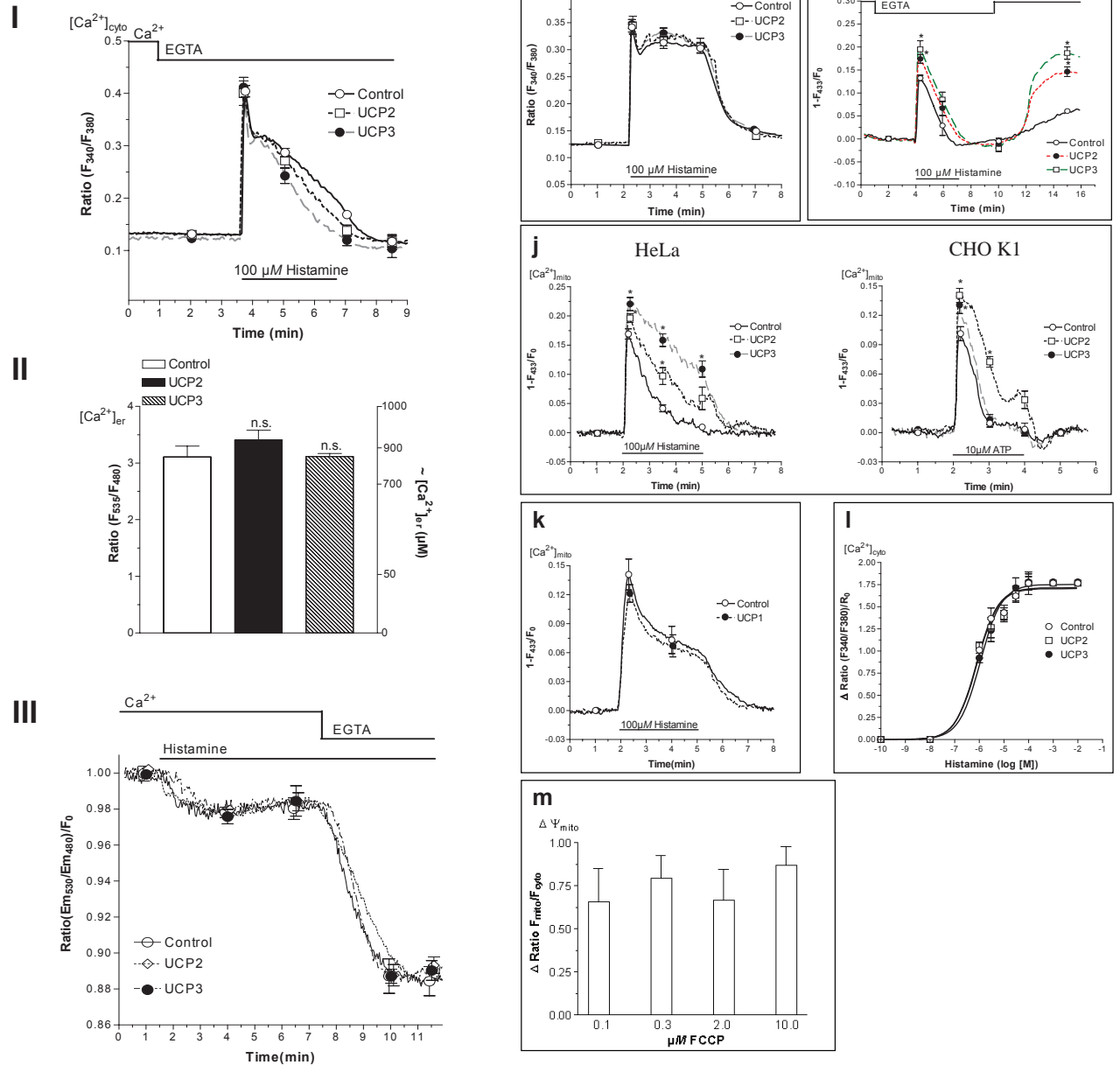


Figure S1. Expression profiling, functional testing and comparison with UCP1.

1a Profile of UCP expression in various freshly isolated human endothelial cells.

Overview of the detection of UCP mRNAs in various cell types (left upper panel). For mRNA detection of the UCP family members, RT-PCRs were performed according to standard procedures using the detection primers given in the left lower panel. The right panels show the agarose gels of the respective cells.

1b. Overexpression of either UCP2 or UCP3 did not affect the architectural organisation of mitochondria in EA.hy926 cells. For the overexpression of UCP2 or UCP3 in double labelling experiments, cells were transiently transfected with 2 μg DNA/ml of YC4er (ER in green) in pcDNA3 and mitochondria-targeted DsRed (mitochondria in red) (Control, left panels) or together with either UCP2 (middle panels) or UCP3 (right panels) that were cloned into the two multicloning sites of pBudCE4.1. 48 h after transfection, z-scans were performed using an array confocal laser scanning microscope (ACLSM) and 3D-reconstruction and focal contact analysis were performed (see Methods section). Upper panels show representative overlay images of ER and mitochondria, middle panels show the mitochondria with focal contact areas with the ER in yellow, and lower panels show the ER with focal contact areas with mitochondria in yellow. The statistical evaluation of the focal contacts between the mitochondria and the ER are presented in Suppl. Fig. 1e.

1c-I: Expression of UCP2 or UCP3 did not affect the Ca^{2+} dynamic of the Ca^{2+} -sensitive wavelengths (F_{433}) of mitochondria-targeted pericam. Basal, maximal and minimum F_{433} signals of mitochondria-targeted pericam were obtained in single endothelial cells that were transiently transfected with either the vector alone (Control, white columns, $n=15$), UCP2 (black columns, $n=7$) or UCP3 (grey columns, $n=9$). After monitoring the basal value, minimum and maximum F_{433} values were measured in high KCl buffer (in mM: 135 KCl, 10 NaCl, 1 MgCl_2 , 20 Hepes; pH 7.7) under nominal Ca^{2+} free (1 mM EGTA; minimum) and saturating high Ca^{2+} conditions (10 mM; maximum) in the presence of 5 μM ionomycin, 5 μM digitonin, 4 μM FCCP and 2 μM oligomycin.

1c-II: Mitochondrial matrix pH remained unchanged by overexpression of UCP2 or UCP3. To estimate whether or not overexpression of UCP2 or UCP3 affects basal pH in the mitochondria human endothelial cells were transiently transfected with mitochondria-targeted ratiometric pericam (Control, $n=14$) or cotransfected with mitochondria-targeted ratiometric pericam and UCP2 ($n=11$) or UCP3 ($n=14$). Mitochondrial pH was monitored using the pH-sensitive wavelength of mitochondria-targeted ratiometric pericam (i.e. 485 nm excitation)¹. Mitochondria were acidified with 2 μM FCCP in the presence of 2 μM oligomycin and 10 μM CGP 37157 an inhibitor of mitochondrial $\text{Na}^+/\text{Ca}^{2+}$ exchanger ($n=14$ different experiments).

1d. Overexpression of either UCP2 or UCP3 did not affect the membrane potential of the inner mitochondrial membrane (ψ_{mito}) in EA.hy926 cells. As the fluorescence of mitochondrially accumulated JC-1 is proportional to the mitochondrial membrane potential² this potentiometric dye was used to assess ψ_{mito} . In endothelial cells expressing either mitochondria-targeted DsRed alone or together with UCP2 or UCP3 the intracellular distribution of JC-1 was assessed by confocal microscopy (*panel I*, ACLSM, see Methods section). Addition of 40 nM JC-1 to the perfusion medium caused a rapid accumulation of this dye within mitochondria, whereas the fluorescence of JC-1 only slowly increased to a much lesser extent in extra-mitochondrial areas of the cell. Upon addition of 2 μM of the chemical uncoupler FCCP after JC-1 loading a fast redistribution of the potentiometric dye from mitochondria to extra-mitochondrial areas could be observed (*panel II*). Consequently, the ratio between the average intensity of the JC-1 fluorescence within mitochondria (F_{mito}) and of an extra-mitochondrial area (F_{cyto}) was used as an indicator of ψ_{mito} which is independent of dye-loading, light scattering and other optical factors. Neither overexpression of UCP2 nor that of UCP3 affected the intracellular distribution of JC-1 under basal conditions (Control $n=12$, UCP2 $n=9$, UCP3 $n=11$, -FCCP). In line with this finding, addition of FCCP resulted in an equal decline of the $F_{\text{mito}}/F_{\text{cyto}}$ ratio regardless of the UCP2/3 expression levels (Control $n=5$, UCP2 $n=4$, UCP3 $n=7$, +FCCP) (*panel III*). These measurements clearly indicate that under basal conditions ψ_{mito} is not affected by UCP2 or UCP3 overexpression in the endothelial cells used within this study. In an analogous manner $F_{\text{mito}}/F_{\text{cyto}}$ ratio values were obtained in the presence of histamine (100 μM) and histamine plus FCCP, indicating that under condition of cell stimulation with an IP_3 generating agonist, ψ_{mito} is also not modified by an overexpression of either UCP2 or UCP3 (numbers of experiments: Control, $n=7$; UCP2, $n=5$; UCP3, $n=5$; + Histamine and Control, $n=7$; UCP2, $n=5$; UCP3, $n=5$; +Histamine / FCCP, $n=5$) (*panel IV*).

1e. Basal ATP concentration in endothelial cells was not affected by overexpressing UCP2 or UCP3. A, Endothelial cells were transiently transfected with cytosolic luciferase together with either mitochondria-targeted DsRed alone (Control, $n=7$) or with UCP2 ($n=7$) or UCP3 ($n=7$). After the addition of 40 μM luciferin, bioluminescence that reflects cytosolic ATP concentration was monitored in cell monolayers.

1f. Overexpression of either UCP2 or UCP3 did not affect the focal contacts of mitochondria with the ER in EA.hy926 cells. Overexpression of neither UCP2 nor UCP3 changed the percentage of focal contacts of the ER with mitochondria and the fraction of mitochondria that co-localised with the ER (Supp. Fig. 1b; Control: $n=22$; UCP2: $n=6$; UCP3: $n=22$; $0.31 < p > 0.65$). The respective volumes of co-localisation, where due to the optical resolution of the system an explicit discrimination of the two organelles could not be achieved, are represented in yellow combined with mitochondria (red) or ER (green) in the middle and right panels, respectively. These focal contacts between ER and mitochondria were defined as the percentage values of voxels that contain both fluorescent proteins, which were obtained from the co-localisation analysis module in Imaris 3.3. The surface area and the volume of mitochondria per cell were not affected by overexpression of either UCP2 or UCP3 (*panel I*; Control: $n=22$; UCP2: $n=6$; UCP3: $n=22$; $0.09 < p > 0.20$). The interconnected, tubular appearance of mitochondria within individual endothelial cells and the number of single mitochondria per cell were also not altered by overexpression of these UCP orthologs. In contrast to the overexpression of UCP2 and UCP3, the chemical uncoupler FCCP (2 μM) initiated fragmentation of mitochondria within 5 minutes (*panel II*). FCCP treatment significantly increased the number of single mitochondria per cell from 83 ± 15 to 159 ± 15 in control cells ($n=10$) and from 90 ± 16 to 143 ± 21 in cells overexpressing UCP3 ($n=8$) within 5 minutes (*panel III*). “n” values indicate the number of cells from at least three different experiments.

1g. Basal ER Ca^{2+} content and histamine-induced Ca^{2+} release remained unchanged by overexpression of UCP2 or UCP3. *Panel I:* Endothelial cells were transiently transfected with mitochondria-targeted DsRed alone (Control, $n=11$) or together with UCP2 ($n=12$) or UCP3 ($n=12$), loaded with fura-2/am (see Methods) and cytosolic Ca^{2+} elevations in response to 100 μM histamine in the nominal absence of extracellular free Ca^{2+} (i.e. no Ca^{2+} added plus 1 mM EGTA) were fluorometrically recorded in single cells. *Panel II and III:* Endothelial cells were transfected with D1ER, an ER targeted FRET based Ca^{2+} sensor. The basal F_{535}/F_{480} ratio of this ratiometric ER Ca^{2+} sensor was not affected upon overexpression of either UCP2 or UCP3 (Control: $n=6$; UCP2: $n=5$; UCP3: $n=6$) indicating that the global ER Ca^{2+} content under basal conditions was not altered by an overexpression of these UCP-orthologs. In line with these results histamine induced ER Ca^{2+} depletion was identical in control cells ($n=6$), UCP2 overexpressing cells ($n=5$) and UCP3 overexpressing cells ($n=6$) in the presence as well as in the absence of extracellular Ca^{2+} . “n” values indicate the number of cells from at least three different experiments.

1h. Cytoplasmic Ca^{2+} elevation in response to histamine was not affected in UCP overexpressing cells. Endothelial cells were transiently transfected with either mitochondria-targeted DsRed alone (Control, $n=17$), or together with UCP2 ($n=21$) or UCP3 ($n=16$), loaded with fura-2/am (see Methods) and cytosolic Ca^{2+} elevations in response to $100 \mu\text{M}$ histamine in the presence of 2 mM free extracellular Ca^{2+} were fluorometrically recorded in single cells. “ n ” values indicate the number of cells from at least ten different experiments.

1i. Increased mitochondrial Ca^{2+} sequestration in UCP overexpressing cells was independent from the source of Ca^{2+} . Endothelial cells were transiently transfected with mitochondria-targeted ratiometric pericam alone (Control, $n=9$) or together with UCP2 ($n=9$) or UCP3 ($n=9$). Mitochondrial Ca^{2+} concentration was recorded in single cells as described under Methods. As indicated, cells were stimulated with $100 \mu\text{M}$ histamine in the absence of extracellular Ca^{2+} followed by readdition of 2 mM extracellular Ca^{2+} . * $P>0.05$ vs control. “ n ” values indicate the number of different experiments.

1j. As in endothelial cells, overexpression of UCP2 or UCP3 yielded increased mitochondrial Ca^{2+} sequestration in HeLa and CHO-K1 cells. HeLa (*left panel*) and CHO-K1 (*right panel*) cells were transiently transfected with mitochondria-targeted ratiometric pericam alone (Control, HeLa: $n=11$; CHO-K1: $n=13$) or together with UCP2 (HeLa: $n=9$; CHO-K1: $n=10$) or UCP3 (HeLa: $n=10$; CHO-K1: $n=11$). As indicated, HeLa and CHO-K1 cells were stimulated with $100 \mu\text{M}$ histamine or $10 \mu\text{M}$ ATP, respectively. * $P>0.05$ vs control. “ n ” values indicate the number of cells from at least six different experiments.

1k. Expression of UCP1 did not affect mitochondrial Ca^{2+} sequestration upon stimulation with an agonist. EA.hy926 cells were transiently transfected with mitochondria-targeted ratiometric pericam alone (Control, $n=13$) or together with UCP1 ($n=15$). As indicated, cells were stimulated with $100 \mu\text{M}$ histamine. Mitochondrial Ca^{2+} concentration was recorded in single cells as described under Methods. “ n ” values indicate the number of cells from at least six different experiments.

1l. The efficiency of histamine to elevate cytosolic Ca^{2+} was not affected by overexpression of UCPs. EA.hy926 cells were transiently transfected with mitochondria-targeted DsRed alone (Control, $n=6-12$) or together with UCP2 ($n=6-12$) or UCP3 ($n=6-12$), loaded with fura-2/am (see Methods) and cytosolic Ca^{2+} elevations in response to various concentrations of histamine ($10^{-8} - 10^{-2} \text{ M}$) in the presence of 2 mM free extracellular Ca^{2+} were fluorometrically recorded in single cells. “ n ” values indicate the number of cells from at least three different experiments.

1m. Efficiency of FCCP to depolarize mitochondria in the endothelial cells. In order to assess whether or not $2 \mu\text{M}$ FCCP is enough to completely degrade ψ_{mito} within 3 minutes in the respective cell model (see mitochondrial Ca^{2+} uptake under depolarizing conditions Fig. 1e) different concentrations of FCCP from 0.1 to $10 \mu\text{M}$ were used and JC-1 redistribution was monitored as described in Suppl. Fig. 1d. $\Delta \psi_{\text{mito}}$ did not significantly change upon increasing the FCCP concentration from 0.1 to $10 \mu\text{M}$ ($n=3$ for each concentration) indicating that within 3 minutes the maximal effect of FCCP on ψ_{mito} was achieved with the usage of $2 \mu\text{M}$ of this chemical uncoupler.

Suppl. Fig. 3

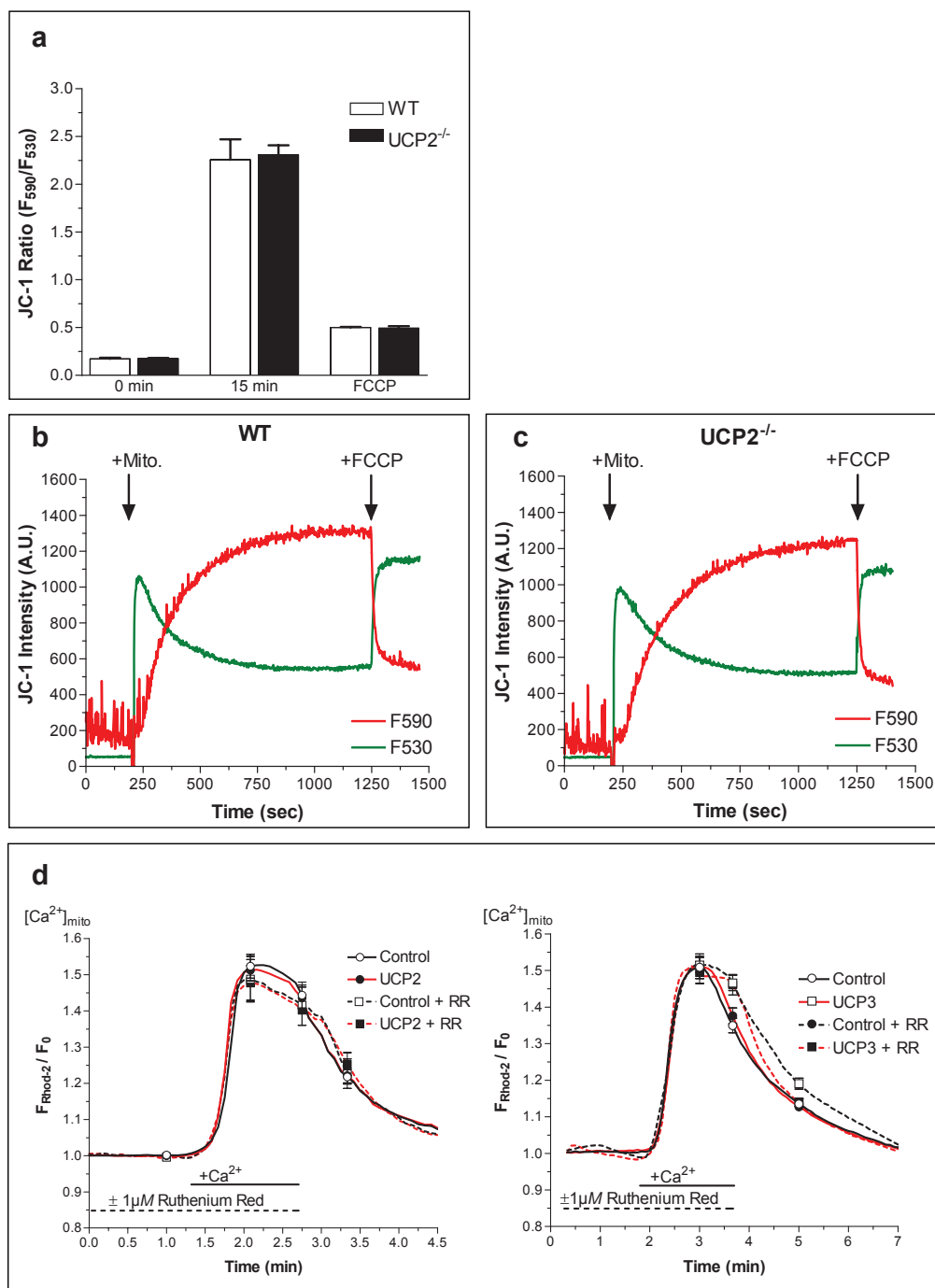


Figure S3. Concerning data in single liver mitochondria from wild type and UCP2^{-/-} mice (panels a-c), and single mitochondria freshly isolated from wild type yeast, and UCP2 and UCP3 expressing yeast (panel d). **3a-c:** No difference in the membrane potential of suspended liver mitochondria between organelles isolated from wild type and UCP2^{-/-} mice was observed. The membrane potential of suspended mitochondria freshly isolated from wild type and UCP2^{-/-} mice was measured using JC-1 as in Methods. Panel a shows the statistical summary of all experiments performed (WT, n=6) and UCP2^{-/-} (n=6). Panel b and c are representative tracings where suspended mitochondria were added to the JC-1 containing solution as indicated. In order to evaluate the fluorescence at 0 mV membrane potential 4 μM FCCP were added after the JC-1 signal reached a stable plateau phase.

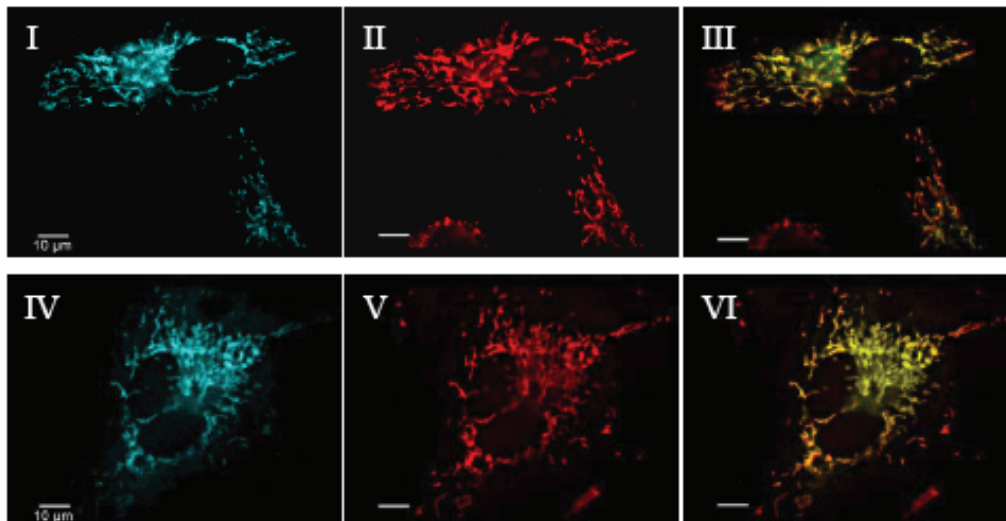
3d. Comparison of mitochondrial Ca²⁺ sequestration and its sensitivity to ruthenium red in freshly isolated single mitochondria from wild type yeast, and yeast expressing either UCP2 and UCP3. Ca²⁺ uptake in isolated single mitochondria from *Saccharomyces cerevisiae* diploid, W303 (a/α), transformed with either the plasmid vector pRUCP2 (moderate UCP2 expression) (left panel: UCP2, n=54) or with the pYes2 empty vector as the paired control³ (left panel: Control, n=52), or with either the plasmid vector pBF354 (UCP3 expression) (right panel: UCP3, n=44) or with pKV49 (empty vector control)⁴ (right panel: Control, n=47). After loading with rhod-2 (see Methods below) mitochondrial Ca²⁺ sequestration upon addition of 10 μM free Ca²⁺ was monitored fluorometrically in the absence or presence of 1 μM ruthenium red (+RR).

Suppl. Fig. 4

a

Predicted Domain	UCP	Aminoacids	Sequence	AA Identity / Homology (%)
Transmembrane domain 1	UCP1	17-34	LFSAPIAACLADVITFPL	UCP1:UCP2 11 / 61
	UCP2	17-34	FLGAGTAACIADLITFPL	UCP1:UCP3 10 / 56
	UCP3	17-34	FLGAGTAACFADLVTFPL	UCP2:UCP3 16 / 89
Transmembrane domain 2	UCP1	77-96	GLPAGLQRQISSASLRIGLY	UCP1:UCP2 16 / 80
	UCP2	81-100	GLVAGLQRQMSFASVRIGLY	UCP1:UCP3 16 / 80
	UCP3	80-99	GLVAGLQRQMSFASIRIGLY	UCP2:UCP3 19 / 95
Transmembrane domain 3	UCP1	115-134	SKILAGLTTGGVAVFIGQPT	UCP1:UCP2 12 / 60
	UCP2	118-137	SRLLAGSTTGALAVAVAQPT	UCP1:UCP3 12 / 60
	UCP3	118-137	TRILAGCTTGAMAVTCAQPT	UCP2:UCP3 14 / 70
Transmembrane domain 4	UCP1	176-195	GTFPNLMRSVIINCTELVTY	UCP1:UCP2 13 / 65
	UCP2	178-197	GTSPNVARNAIVNCBELVTY	UCP1:UCP3 13 / 65
	UCP3	181-200	GTLPNIMRNAIVNCAEVVTY	UCP2:UCP3 16 / 80
Transmembrane domain 5	UCP1	215-233	HLVSALIAGFCATAMSSPV	UCP1:UCP2 11 / 58
	UCP2	217-235	HFTSAFGAGFCTTVIASPV	UCP1:UCP3 13 / 68
	UCP3	220-238	HFVSAFGAGFCATVVASPV	UCP2:UCP3 16 / 84
Transmembrane domain 6	UCP1	270-289	GLVPSFLRLGSWNVIMFVCF	UCP1:UCP2 15 / 75
	UCP2	272-291	GFMPFSLRLGSWNVVMEVTY	UCP1:UCP3 16 / 76
	UCP3	275-294	GFTPSFLRLGSWNVVMEVTY	UCP2:UCP3 19 / 95
Intermembranous loop 1	UCP1	60-70	GTITAVVKTGEG	UCP1:UCP2 7 / 64
	UCP2	64-74	GTILTMVRTEG	UCP1:UCP3 7 / 64
	UCP3	63-73	GTILTMVRTEG	UCP2:UCP3 11 / 100
Intermembranous loop 2	UCP1	157-169	TYNAYRIIATTEG	UCP1:UCP2 8 / 62
	UCP2	159-171	TVNAYKTIAREEG	UCP1:UCP3 8 / 62
	UCP3	162-174	TMDAYRTIAREEG	UCP2:UCP3 10 / 77
Intermembranous loop 3	UCP1	252-264	PNCAMKVFTNEGP	UCP1:UCP2 5 / 38
	UCP2	254-266	GHCALTMLQKEGP	UCP1:UCP3 5 / 38
	UCP3	257-269	LDCMIKMQAQEGP	UCP2:UCP3 5 / 38

b



Suppl. Fig. 4

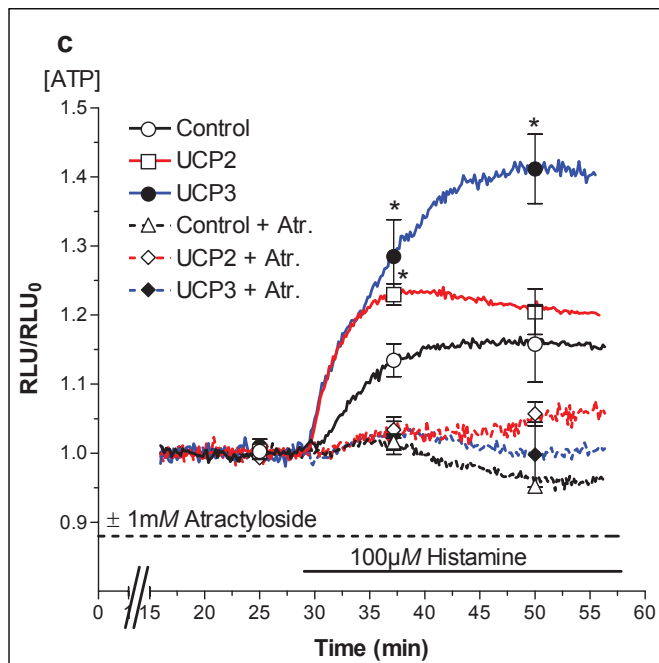


Figure S4. Concerning mutagenesis of the UCP2 and UCP3 (panel a & b) and the effect of UCP2 and UCP3 overexpression on basal (c) and agonist (d)-induced ATP synthesis in the mitochondria. **4a.** Comparison of the amino acid sequence homology between UCP1, UCP2 and UCP3. Amino acid sequences of UCP1, UCP2 and UCP3 were aligned according to the predicted transmembrane and intermembranous loop domains and the sequences and homology are presented. The highlighted sequences indicate the area of highest diversity between UCP2/UCP3 and UCP1 in terms of amino acid properties. This area was emphasized to be important for the Ca^{2+} carrier function of UCP2 and UCP3 and, thus, was selected for mutation. **4b.** Like their non-mutant homologues, the mutated UCP2 and UCP3 were localized exclusively in the mitochondria. Fusion constructs of mutated UCP2 (upper panels) or mutated UCP3 (middle panels) with

sapphire⁵ were expressed and their co-localization with mito-tracker orange[®] was visualized in human endothelial cells. Panels I and IV show the localization of the fusion constructs of mutated UCP2 and mutated UCP3, II and V the localization of mito-tracker orange[®], and III and VI the co-localization in the respective cell. **4c.** Consequently to the mitochondrial Ca^{2+} carrier function of UCP2 and UCP3, agonist-induced mitochondrial ATP production was elevated in UCP overexpressing cells. Endothelial cells were transiently transfected with cytosolic luciferase together with mitochondria-targeted DsRed (Control, n=7), the mitochondria-targeted DsRed and UCP2 (n=7) or the mitochondria-targeted DsRed and UCP3 (n=7). After the addition of 40 μM luciferin bioluminescence was monitored in cell monolayers in the absence or presence of 1 mM attractylolide. * $P < 0.05$ vs Control.

Movie 1: Overexpression of UCP2 and UCP3 did not affect basal mitochondrial dynamics, fusion and fission.

Time scan acquisitions of mitochondrial movement, fusion and fission were performed in cells transiently expressing mitochondria-targeted DsRed (Control) or mitochondria-targeted DsRed and UCP2 (co-transfection) using the ACLSM as described in the Methods section below. At a constant z-plane, images were recorded every 2 s. Exposure time was 1 s. Arrows indicate typical branching of tubular mitochondrial structures. Fluctuations are possibly due to i, small alterations of the z-stage of the motorized microscope, ii, floating cell debris or iii, alterations in the laser power during the experiments.

Movie 2: Ca^{2+} measurements in single mitochondria freshly isolated from yeast *Saccharomyces cerevisiae* using rhod-2.

Changes in rhod-2 fluorescence upon increasing the Ca^{2+} concentration in the buffer from nominal Ca^{2+} free buffer to 10 μM Ca^{2+} were recorded every 5 s using high resolution CCD camera (CoolSnap HQ, Roper Scientific, Visitron Systems, Puchheim, Germany) (for details see Methods below).

Fig. 1c	Control		UCP2		UCP3			
	F_{433}	$R(F_{485}/F_{433})$	F_{433}	$R(F_{485}/F_{433})$	F_{433}	$R(F_{485}/F_{433})$		
	232.2±7.3	0.903±0.016	218.2±9.8	0.917±0.014	217.4±9.6	0.909±0.016		
Fig. 1f	Control		UCP2		UCP3			
	F_{433}	$R(F_{485}/F_{433})$	F_{433}	$R(F_{485}/F_{433})$	F_{433}	$R(F_{485}/F_{433})$		
	226.4±9.3	0.896±0.021	232.2±9.4	0.904±0.017	228.3±9.1	0.907±0.016		
Fig. 2b	Control		siUCP2		siUCP3		siUCP2/3	
	F_{433}	$R(F_{485}/F_{433})$	F_{433}	$R(F_{485}/F_{433})$	F_{433}	$R(F_{485}/F_{433})$	F_{433}	$R(F_{485}/F_{433})$
	253.8±15.5	0.974±0.042	261.8±19.4	0.935±0.038	258.9±23.0	0.954±0.045	260.9±15.1	0.981±0.036
Fig. 2c	Control		siUCP2		siUCP3			
	F_{433}	$R(F_{485}/F_{433})$	F_{433}	$R(F_{485}/F_{433})$	F_{433}	$R(F_{485}/F_{433})$		
	212.6±15.6	0.931±0.016	220.9±11.8	0.942±0.013	221.0±15.3	0.925±0.014		
Fig. 2d	Control		siUCP3		UCP2 + siUCP3			
	F_{433}	$R(F_{485}/F_{433})$	F_{433}	$R(F_{485}/F_{433})$	F_{433}	$R(F_{485}/F_{433})$		
	220.9±18.0	0.920±0.022	238.1±15.2	0.925±0.017	219±8.3	0.941±0.011		
Fig. 4c	Control		mut-UCP2		Control		mut-UCP3	
	F_{433}	$R(F_{485}/F_{433})$	F_{433}	$R(F_{485}/F_{433})$	F_{433}	$R(F_{485}/F_{433})$	F_{433}	$R(F_{485}/F_{433})$
	149.0±4.1	0.958±0.010	157.4±5.6	0.950±0.013	150.2±4.4	0.955±0.011	156.3±5.3	0.941±0.010
Fig. 4d	Control		siUCP3		mut-UCP2 + siUCP3			
	F_{433}	$R(F_{485}/F_{433})$	F_{433}	$R(F_{485}/F_{433})$	F_{433}	$R(F_{485}/F_{433})$		
	530.0±36.3	0.696±0.030	504.3±44.7	0.706±0.023	392.4±22.8	0.731±0.014		
Suppl. Fig. 1h	Control		UCP2		UCP3			
	F_{433}	$R(F_{485}/F_{433})$	F_{433}	$R(F_{485}/F_{433})$	F_{433}	$R(F_{485}/F_{433})$		
	191.0±13.2	0.953±0.022	194.2±18.2	0.937±0.024	195.8±12.1	0.945±0.027		
Suppl. Fig. 1i	Control		UCP2		UCP3			
	F_{433}	$R(F_{485}/F_{433})$	F_{433}	$R(F_{485}/F_{433})$	F_{433}	$R(F_{485}/F_{433})$		
<i>HeLa</i>	173.1±7.6	0.982±0.011	172.2±10.3	0.969±0.013	177.1±13.7	0.981±0.009		
<i>CHO XI</i>	Control		UCP2		UCP3			
	F_{433}	$R(F_{485}/F_{433})$	F_{433}	$R(F_{485}/F_{433})$	F_{433}	$R(F_{485}/F_{433})$		
	317.0±18.6	1.029±0.026	321.5±26.6	1.007±0.018	332.1±36.7	1.006±0.020		
Suppl. Fig. 1j	Control		UCP1					
	F_{433}	$R(F_{485}/F_{433})$	F_{433}	$R(F_{485}/F_{433})$				
	234.3±7.8	0.910±0.013	237.2±7.5	0.921±0.016				

Table S1. Non-normalized original data of the mitochondria-targeted ratiometric pericam data provided in the article. The fluorescence of mitochondria-targeted ratiometric pericam at two different excitation wavelengths is mainly Ca^{2+} - (F_{433}) as well as pH- (F_{485}) dependent. Consequently, caution is necessary when presenting ratiometric data under dynamical conditions in which also changes in the pH might occur. Therefore, to demonstrate changes in mitochondrial Ca^{2+} upon

cell stimulation data are given as $1-F_{433}/F_0$. However, since other basal parameters of mitochondria (see Suppl. Fig. 1) did not alter when UCP2 and UCP3 expression was modulated, a statistical evaluation of the original basal data is shown here in order to conclude that there are no differences in basal mitochondrial Ca^{2+} concentration under conditions of various UCP expression. “n” values correspond to the respective figures.

MATERIALS:

If not indicated separately, all cell culture chemicals and pBudCE4.1 were obtained from Invitrogen Corp. (Carlsbad, California, USA) and fetal calf serum (FCS) was from PAA Laboratories (Linz, Austria). Calcium Gree-5N hexapotassium salt, fura-2/am, 5,5',6,6'-tetrachloro-1,1',3,3'-tetraethyl-benzimidazolcarbocyanine iodide (JC-1) and mito-Tracker Orange[®] were from Molecular Probes Europe (Leiden, Netherlands). ATP, antimycin A, oligomycin, atractyloside, FCCP, histamine, EGTA, luciferin, Ham's F12 and Dulbecco's minimum essential medium (DMEM) were from Sigma-Aldrich (Vienna, Austria). CGP 37157 was from Tocris Cookson Ltd. (Northpoint, Avonmouth, Bristol, UK). Endothelial growth medium (EGM) and the bullet-kit were purchased from Cambrex-Clonetics (Verviers, Belgium). Restriction enzymes and T4 DNA ligase were from Promega (Mannheim, Germany), the EndoFree Plasmid Maxi Kit and the double stranded RNA for UCP3 silencing were from Quiagen (Hilden, Germany). All other chemicals were from Roth (Karlsruhe, Germany). The primary antibodies and ECL solution were purchased from Santa Cruz (UCP2, sc-6525; UCP3, sc-7756; Santa Cruz Biotechnology Inc., Szabo-Scandic, Vienna, Austria) and from Abcam[®] (β -Actin, ab8224; Abcam, Cambridge, UK). As secondary antibodies, peroxidase-conjugated IgGs (rabbit anti-goat IgG, sc-2768, Santa Cruz and rabbit anti-mouse IgG, P 0260, DAKO, Denmark) were used.

METHODS:**Concerning experiments with cultured cells:**

Ψ_{mito} Measurement. Cells expressing mitochondria-targeted DsRed were loaded with 40 nM JC-1 on the ACLSM using a gravity based perfusion system (for details see Methods below). JC-1 was continuously present throughout all the experiments in order to counteract possible leakage of the potentiometric dye. Mitochondria-targeted DsRed and JC-1 were excited with the 488 nm Ar-laser line and emission was alternatively monitored every 0.8 s at 570 nm (for mitochondria-targeted DsRed) and 535 nm (for JC-1). The mitochondria-targeted DsRed channel was used to define regions that cover exclusively mitochondria within one given cell.

The average intensity of the JC-1 fluorescence of this regions (F_{mito}) was divided by the average intensity of the JC-1 fluorescence of a region that was at least 3 μm away from these organelles (F_{cyto}). The $F_{\text{mito}}/F_{\text{cyto}}$ -ratio was used to assess changes in Ψ_{mito} .

Confocal imaging and 3D rendering. Z-scans were performed in cells that were co-transfected with YC4er and mitochondria-targeted DsRed using a *Nipkow*-disk-based array confocal laser scanning microscope (ACLSM)^{6,7}. The ACLSM was built on a Zeiss Axiovert 200M (Zeiss Microsystems, Jena, Germany) equipped with VoxCell Scan[®] (VisiTech, Sunderland, UK), a 150 mW Ar laser (Laser Physics; West Jordan, UT, USA) and controlled by Metamorph 6.2r6 (Universal Imaging, Visitron Systems, Puchheim, Germany). The green fluorescent probe targeted to the ER (i.e. YC4er) and the red fluorescence within mitochondria (i.e. mitochondria-targeted DsRed) were alternatively imaged with a 100 x objective (α Plan-Fluar 100 x / 1.45 oil objective, Zeiss Microsystems, Jena, Germany) using the 488 nm and 514 nm Ar-laser lines for illumination. Z-interval between the planes was 0.1 μm . The emitted light was filtered at 535 nm and 570 nm using two different emission filters (535/30 and E570LPv2, Chroma Technology Corp., Rockingham, VT, USA), which were mounted in a computer-controlled fast filter wheel (Ludl, Electronic Products, Hawthorne, NY, USA). The ER and mitochondria z-stacks were deconvoluted using the iterative quick maximum likelihood estimation algorithm (QMLE) of Huygens 2.4.1p3 (SVI, Hilversum, Netherlands). Subsequently combined 3-D rendering of the organelles, co-localisation analysis, and mitochondrial surface and volume calculations were performed with Imaris 3.3 software (Bitplane AG, Zürich, Switzerland). The intensity threshold values for 3D image restorations and co-localisation computations did not significantly differ within all the samples analysed and were determined over a range that completely eliminated background fluorescence but preserved organelle structures. Focal contacts between ER and mitochondria were defined as the percentage values of voxels that contain both fluorescent proteins, which were obtained from the co-localisation analysis module in Imaris 3.3. Notably, due to the limitation in regard to the optical resolution the percentage values for focal contacts between the ER and mitochondria and vice versa are probably overestimated.

Luminescent ATP assays. Bioluminescent measurements of cellular ATP levels were performed according to Jouaville et al.⁸ All luminescence experiments were performed in a GLOMAX luminometer with 10-seconds integration time (Turner Biosystems, Inc., CA, USA). For intracellular ATP measurements, EA.hy926 cells were seeded on 3cm plates one day before transfection. Cells at app. 80 % confluency were co-transfected with cytosolic luciferase and mitochondria-targeted DsRed for control experiments or co-transfected with cytosolic luciferase and UCP2 or UCP3 mitochondria-targeted DsRed for UCP-overexpressor experiments. 48 h after transfection cells were washed twice with HEPES-buffered Ca^{2+} solution (EB) and measurement of luminescence was started after adding 40 μM luciferin. 100 μM histamine was added 30 min past start. As indicated, 1mM atractyloside was applied to the cells.

Concerning the experiments in single and suspended liver mitochondria freshly isolated from wild type and knockout mice:

Isolation of mitochondria from mouse liver. Liver mitochondria from wild-type (WT) and UCP2 knock-out (UCP2^{-/-}) mice were isolated by differential centrifugation as described by Storrie and Madden⁹ followed by a sucrose-gradient centrifugation to further purify the mitochondrial fraction. Shortly, the fresh tissue sample was washed twice with 2 volumes of extraction buffer EB (in mM: 10 HEPES, 250 sucrose and 1 EGTA, pH 7.5), cut into small slices and homogenized in 10 ml EB per g tissue containing 2 mg/ml BSA in a Potter homogenizer with a Teflon pestle (B. Braun, Melsungen, Germany). To separate the mitochondria from other organelles and cell debris the homogenate was centrifuged at different speeds. The obtained raw mitochondrial pellets were then placed on top of a 2-step sucrose gradient consisting of a 1.5 M sucrose and a 1.0 M sucrose phase and centrifuged 25 min at 45000 g. Purified mitochondria were collected from the interphase, pelleted and resuspended in storage buffer SB (in mM: 10 HEPES, 250 sucrose, 1 ATP, 0.08 ADP, 5 succinate, 2 KH_2PO_4 , 1 DTT, pH 7.4). All steps were carried out at 0-4°C.

Measurement of the mitochondrial membrane potential. The membrane potential of liver mitochondria isolated from wild-type and UCP2^{-/-} mice was measured on a Hitachi F-4500

fluorescence spectrometer at room temperature using JC-1 (Molecular Probes). 2 μ L of JC-1 (0.2 mg/ml) were added to 2 ml of KCl-buffer (see above). A dual-wavelength program allowed to monitor a time-dependent kinetics of both, the green fluorescent monomers and the red fluorescent J-aggregates, with excitation/emission wavelength of 490nm/530nm and 490nm/590nm, respectively. The ratios between red fluorescence vs. green fluorescence (F_{590}/F_{530}) reflect the mitochondrial loading of JC-1. Following an initial period of incubation, a suspension of isolated mitochondria (0,12 mg of protein) were added to the stirred buffer and the uptake of JC-1 into the mitochondria was monitored in 2 second intervals for up to 20 minutes, since both wavelengths reached a plateau after approx. 15 minutes. At the end of each experiment 4 μ M FCCP was added, leading to a depolarisation of the mitochondria and a drastic decrease of red fluorescence of JC-1 due to equalization of the JC-1 fluorescence inside and outside the mitochondrial matrix.

Concerning the experiments in single mitochondria freshly isolated from yeast

Saccharomyces cerevisiae expressing either UCP2 or UCP3:

Expression of human UCP2 and UCP3 at physiological levels in the yeast *Saccharomyces cerevisiae*. For the expression of human UCP2 and UCP3 in yeast we used cells of the *Saccharomyces cerevisiae* diploid, W303 (a/a), transformed with either the plasmid vector pRUCP2 (moderate UCP2 expression) or with the pYes2 empty vector as the paired control³, or with either the plasmid vector pBF354 (UCP3 expression) or with pKV49 (empty vector control)⁴. Procedures of UCP2 and UCP3 expressions were performed according to the published standard protocols^{3,4}. According to the provider, these procedure yields expression of UCP2 and UCP3 on a similar level in yeast mitochondria as found in mammals¹⁰.

Isolation of mitochondria from *Saccharomyces cerevisiae*. Mitochondria from *Saccharomyces cerevisiae* were isolated as described by Daum et al.¹¹. Cells were harvested at an D_{600} of approx. 2 by centrifugation at 3000 g for 5 min at room temperature, washed once with distilled water, suspended to 0.5 g wet weight/ml in 0.1 M Tris \cdot SO₄, pH 9.4, 10 mM DTT, and incubated for 10 min at 30°C. Subsequently, the cells were re-centrifuged and

washed once, and suspended in 1.2 M sorbitol, 20 mM KH_2PO_4 , pH 7.4, to give 0.15 g cell wet weight/ml. Zymolyase 20T (2 mg/g cell wet weight) was added and the suspension was incubated at 30 °C for 45-60 min. Spheroplasts were pelleted at room temperature, washed with 1.2 M sorbitol and resuspended in ice cold buffer containing 0.6 M mannitol, 10 mM TrisCl, pH 7.4 and 1mM PMSF to a concentration of 0.15 g spheroplasts/ml. All subsequent operations were carried out at 4 °C. Spheroplasts were homogenized by 15 strokes in a Dounce homogenizer. The homogenate was centrifuged for 5 min at 3500 g, the supernatant was saved and the pellet was rehomogenized two times as before. The combined supernatants were centrifuged 10 min at 12000 g to sediment the crude mitochondrial fraction. The pellet was carefully resuspended in homogenisation buffer and centrifuged for 5 min at 3500 g to remove residual cell debris. The supernatant was then centrifuged for 10 min at 12000 g and the final mitochondrial pellet was washed once with PMSF free homogenisation buffer and resuspended in storage buffer SB at a concentration of 8 mg/ml mitochondrial protein.

Loading of yeast mitochondria with rhod-2/am. The mitochondrial suspension with a concentration of approx. 8mg/ml of mitochondrial protein was loaded with 2 μM rhod-2/am for 60 min in the dark at room temperature under continuous stirring. The mitochondria were then washed 2 x with 2 volumes and 1 x with 1 volume SB. Finally, mitochondria were resuspended in assay buffer AB (in mM: 20 Hepes, 130 KCl, 1 MgCl_2 , 0.5 KH_2PO_4 , 10 succinate, 2 malate, 0.5 EGTA, 0.6 ATP, 0.05 ADP, pH 7.2) at a final concentration of 8 mg/ml mitochondrial protein.

Fluorescence measurements of single mitochondria isolated from yeast. Measurements of yeast mitochondria Ca^{2+} signal were performed using rhod-2. Rhod-2-containing organelles were excited at 546 nm (D546/10) and emitted light was collected at >590 nm (e590v2lp; dichroic: 565dclp); 2 s exposure time) upon changing the perfusion solution from Ca^{2+} free buffer (AB) to a 10 μM Ca^{2+} containing buffer (see Movie 2). Experiments were performed using an inverted fluorescence microscope (Zeiss Axiovert 200M) equipped with a 100x oil immersion objective (NA=1.45, Zeiss, Vienna, Austria).

REFERENCES to the supplementary material:

1. Malli, R., Frieden, M., Trenker, M. & Graier, W. F. The role of mitochondria for Ca^{2+} refilling of the ER. *J Biol Chem* 280, 12114-12122 (2005).
2. Szilagyi, G., Simon, L., Koska, P., Telek, G. & Nagy, Z. Visualization of mitochondrial membrane potential and reactive oxygen species via double staining. *Neurosci Lett* 399, 206-209 (2006).
3. Stuart, J. A., Harper, J. A., Brindle, K. M., Jekabsons, M. B. & Brand, M. D. Physiological levels of mammalian uncoupling protein 2 do not uncouple yeast mitochondria. *J Biol Chem* 276, 18633-18639 (2001).
4. Stuart, J. A., Harper, J. A., Brindle, K. M., Jekabsons, M. B. & Brand, M. D. A mitochondrial uncoupling artifact can be caused by expression of uncoupling protein 1 in yeast. *Biochem J* 356, 779-789 (2001).
5. Mizuno, H., Sawano, A., Eli, P., Hama, H. & Miyawaki, A. Red fluorescent protein from *Discosoma* as a fusion tag and a partner for fluorescence resonance energy transfer. *Biochemistry* 40, 2502-2510 (2001).
6. Malli, R., Frieden, M., Osibow, K. & Graier, W. F. Mitochondria efficiently buffer subplasmalemmal Ca^{2+} elevation during agonist stimulation. *J Biol Chem* 278, 10807-10815 (2003).
7. Malli, R. et al. Sustained Ca^{2+} transfer across mitochondria is essential for mitochondrial Ca^{2+} buffering, store-operated Ca^{2+} entry, and Ca^{2+} store refilling. *J Biol Chem* 278, 44769-44779 (2003).
8. Jouaville, L. S., Pinton, P., Bastianutto, C., Rutter, G. A. & Rizzuto, R. Regulation of mitochondrial ATP synthesis by calcium: evidence for a long-term metabolic priming. *Proc Natl Acad Sci U S A* 96, 13807-13812 (1999).
9. Storrie, B. & Madden, E. A. Isolation of subcellular organelles. *Methods Enzymol* 182, 203-225 (1990).
10. Harper, J. A. et al. Artfactual uncoupling by uncoupling protein 3 in yeast mitochondria at the concentrations found in mouse and rat skeletal-muscle mitochondria. *Biochem J* 361, 49-56 (2002).
11. Daum, G., Bohni, P. C. & Schatz, G. Import of proteins into mitochondria. Cytochrome b2 and cytochrome c peroxidase are located in the intermembrane space of yeast mitochondria. *J Biol Chem* 257, 13028-13033 (1982).